Soil Liquefaction/Nonliquefaction in the Achaia-Ilia (Greece) 2008 Earthquake: Field Evidence, Site Characterization and Ground Motion Assessment

***Anastasios Batilas**, M.Sc., Doctoral Student of Civil Engineering, University of Patras, Greece, email:abatilas@upatras.gr*
***Panagiotis Pelekis**, Ph.D., Assoc. Professor of Civil & Structural Engineering, ASPETE, N. Heraklion, Greece, email: pelekis@aspete.gr*
***Vasileios Vlachakis**, M.Sc., Doctoral Student of Civil Engineering, University of Patras, Greece, email: vvlach@upatras.gr*
***George Athanasopoulos**, Ph.D., Professor of Civil Engineering, University of Patras, Greece, email: gaa@upatras.gr*

ABSTRACT*: Macroseismic observations in the meizoseismal area of the Achaia-Ilia, Greece, M_w 6.4 earthquake of 8 June, 2008, have shown that soil liquefaction occurred at a number of sites up to distances of 25 km from the causative fault. In one of these sites (SITE-I at coastal zone of Kato Achaia) the occurrence of liquefaction was extensive and was followed by lateral spreading. In another nearby site (SITE-II) only marginal liquefaction (or nonliquefaction) was observed. Following the macroseismic observations, a geotechnical investigation was carried out at SITE-I and SITE-II which included exploratory boreholes with continuous sampling, SPT measurements, CPT soundings, surface wave measurements (SASW, MASW, ReMi) and laboratory testing. Based on the results of geotechnical investigation, the soil stratigraphy and pertinent soil properties were evaluated in the liquefaction/nonliquefaction locations. The assessment of peak ground acceleration at the area of SITE-I and SITE-II was based on attenuation relations and shaking table tests performed to simulate the observed behavior of an overturned (during the main shock), barrel-shaped, plastic, water filled container sitting on the ground surface at SITE-I. It is believed that the data presented in this paper can be used to 1) check the validity of current liquefaction susceptibility criteria/liquefaction triggering relationships, and 2) establish a well documented liquefaction case history that can be part of future liquefaction databases.*

KEYWORDS: Soil liquefaction, Field observations, Site characterization, Achaia-Ilia Earthquake (2008), Peak ground acceleration.

SITE LOCATION: IJGCH-database.kmz (requires Google Earth)

INTRODUCTION

The damage potential of soil liquefaction–to both infrastructure and residential structures–has been dramatically demonstrated in two recent, strong earthquakes, namely the 2011 East Japan (Tohoku) earthquake (Ishihara, 2012; Yasuda et al., 2012; Tsukamoto et al., 2012; Yamaguchi et al., 2012) and the 2010/2011 Darfield-Christchurch (New Zealand) earthquakes (GEER Report, 2010, 2011; Orense et al., 2012; Cubrinovski et al., 2011). Other recent, strong earthquakes that induced widespread liquefaction, include the 2012 Emilia-Romanga (Northern Italy) earthquake (Lai et al., 2012; Caputo and Papathanassiou, 2012), the 2010 Chile (Maule) earthquake (Verdugo, 2012; GEER Report, 2010) and the 2010, Haiti earthquake (GEER Report, 2010).

It is anticipated that the compilation, study and analysis of the observations made in the above earthquakes–along with data obtained from less recent events–will produce numerous case histories, which will enhance the existing worldwide databases on soil liquefaction. It is known that well documented case histories of earthquake induced soil liquefaction/cyclic softening can provide valuable data for 1) studying the validity of liquefaction susceptibility criteria and relevant triggering conditions, 2) taking into consideration the actual field behavior in terms of void migration (which

Submitted: 27 April 2013; Published: 14 January 2014
Reference: Batilas, A., Pelekis, P., Vlachakis, V., and Athanasopoulos, G. (2014). *Soil Liquefaction/Nonliquefaction in the Achaia-Ilia (Greece) 2008 Earthquake: Field Evidence, Site Characterization and Ground Motion Assessment*. International Journal of Geoengineering Case histories, http://casehistories.geoengineer.org, Vol.2, Issue 4, p.270-287.
doi: 10.4417/IJGCH-02-04-03

cannot be simulated in laboratory testing), 3) for estimating the residual strength of liquefied material or checking the accuracy of available predictive equations for lateral spreading displacements, and 4) for studying the effectiveness of relevant mitigation measures (Idriss and Boulanger, 2008). It is recognized, however, that the value of relevant case histories depends on the available amount of site characterization data (through in situ and laboratory testing) as well as on information regarding the characteristics of earthquake ground motion at the liquefied site (Boulanger and Idriss, 2012; Moss et al., 2011).

The subject of the present study is the presentation of a case history involving soil liquefaction/nonliquefaction and lateral spreading in the coastal zone of Kato Achaia, about 6 km from the causative fault of the Achaia-Ilia (Greece) M_w 6.4 earthquake of June 8, 2008, (Margaris et al., 2008, 2010; Batilas et al., 2011). The M_w 6.4 earthquake of June 8, 2008 in Achaia-Ilia prefecture near the city of Patras, Greece, caused severe damage to buildings and other engineered structures in the meizoseismal area, as well as a variety of geotechnical failures within approximately 25 km from fault (Margaris et al. 2008, 2010). These failures encompass soil liquefaction, with or without lateral spreading, slope instabilities, rockfalls, as well as coastal subsidence phenomena (Figure 1). The present study involves field observations, in-situ geotechnical investigations, laboratory testing, and assessment of the ground motion characteristics at the liquefaction sites of Kato Achaia.

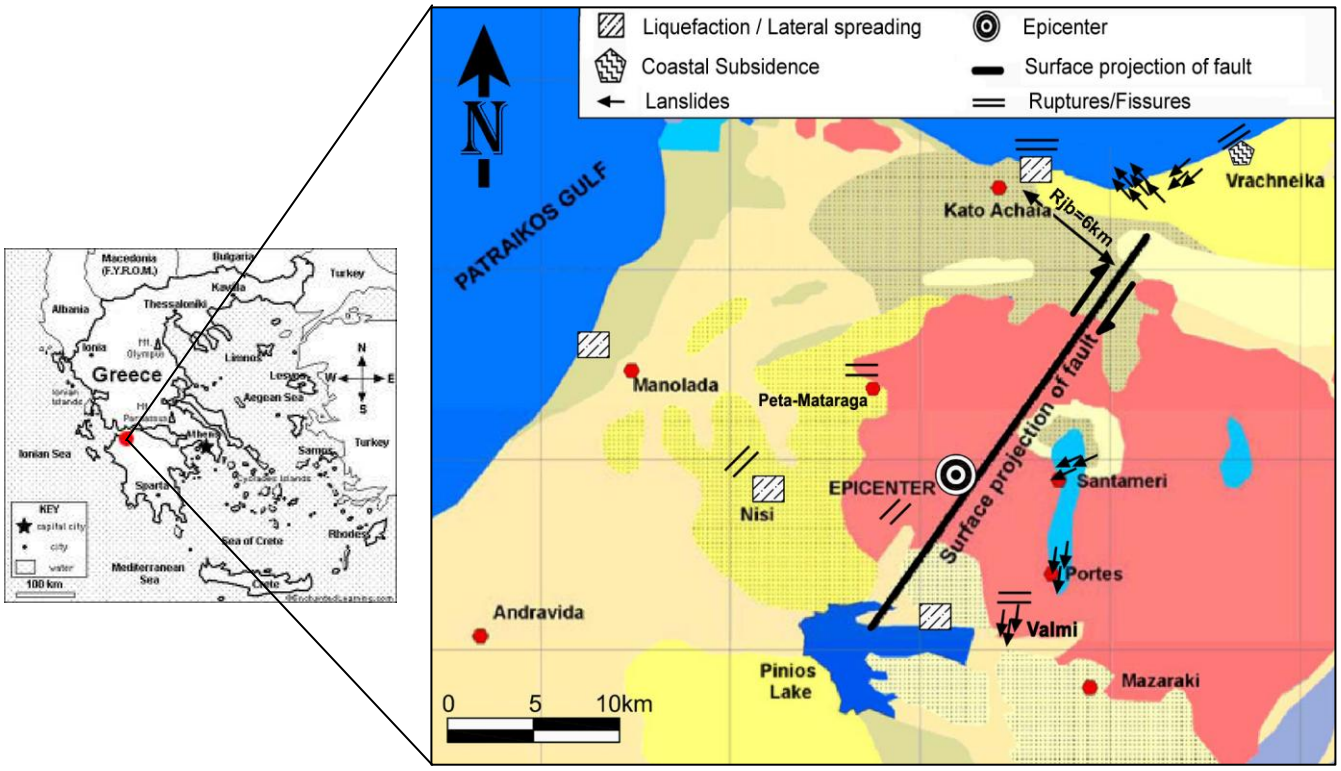

Figure 1. Epicenter, estimated fault trace and locations of ground failure in the June 8, 2008 Achaia-Ilia, earthquake.

FIELD OBSERVATIONS

Post-earthquake reconnaissance in the meizoseismal area was conducted by a team of Greek and U.S. investigators on June 10 and 11, 2008, approximately 48 hours after the main event, and included the recording of the behavior of surface soil formations and topographic mapping of the liquefaction sites. A detailed account of the reconnaissance effort is provided in Margaris et al. (2008, 2010). Two liquefaction/nonliquefaction sites were detected at two nearby locations, to be referred hereafter to as SITE-I and SITE-II.

SITE-I (N38° 09.099′, E21° 33.786′) is located in the coastal zone of Kato Achaia, at a distance of 590 m N-NE from the train station - less than 100 m from the shoreline. It is characterized by a very gentle inclination (≈0.4%) towards the sea-shore (Figure 2). SITE-II (N38° 09.163′, E21° 33.576′) is located 350 m west of SITE-I and possesses similar characteristics.

During the reconnaissance effort, typical features of soil liquefaction were detected on SITE-I, involving sand boils and silty sand ejecta having light brown color and gray color, respectively (Figure 3). In SITE-II the observations showed only marginal liquefaction (or nonliquefaction) with only a single small-sized sand crater with traces of ejecta (Figure 4) found at the location indicated in Figure 2.

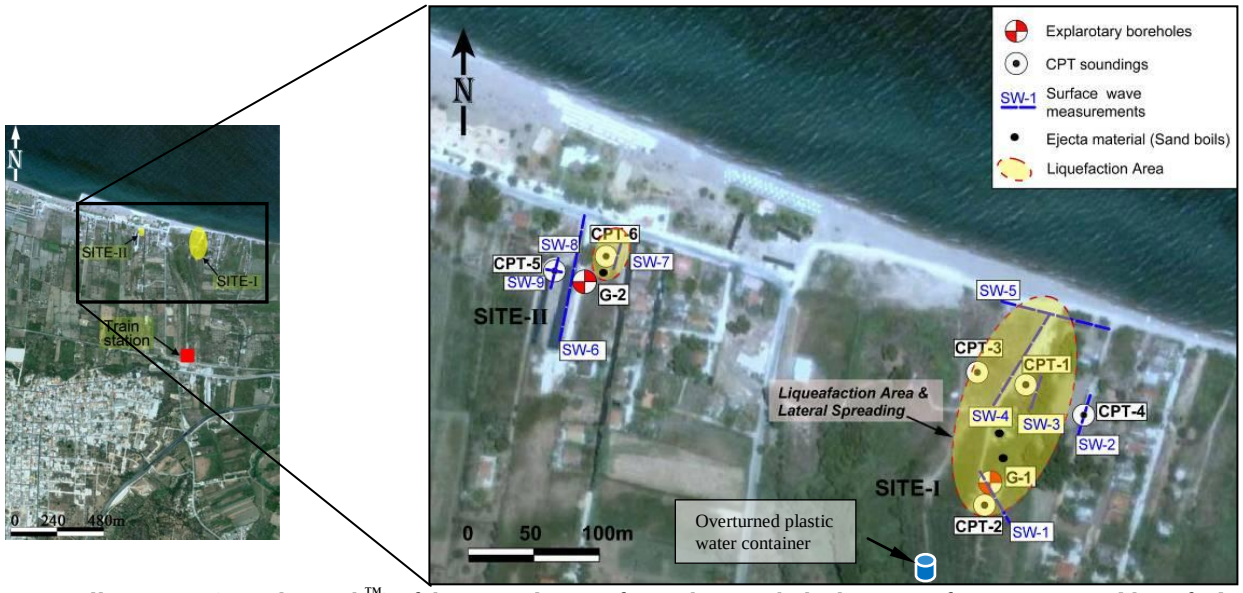

Figure 2. Satellite image (Google Earth™) of the coastal zone of K. Achaia with the location of in situ tests and liquefied areas.

Figure 3. Cone ejecta at SITE-I, in the coastal zone of K. Achaia following the 8-6-2008 earthquake: (a) gray silty sand (SM), (b) brown sand (SP).

Figure 4. Marginal soil liquefaction at SITE-II, in the coastal zone of K. Achaia, following the 8-6-2008 earthquake. The ejected material is clasified as gray silty sand (SM).

The gradation of the ejected materials from SITE-I is depicted in Figure 5: gray material is classified according to USCS as silty sand (SM), having coefficient of uniformity C_u=12.4, C_c=1.38 and 30% content of non-plastic fines. The brown material is classified as fine sand (SP) with C_u=2.91, C_c=1.26 and fines content of about 5%.

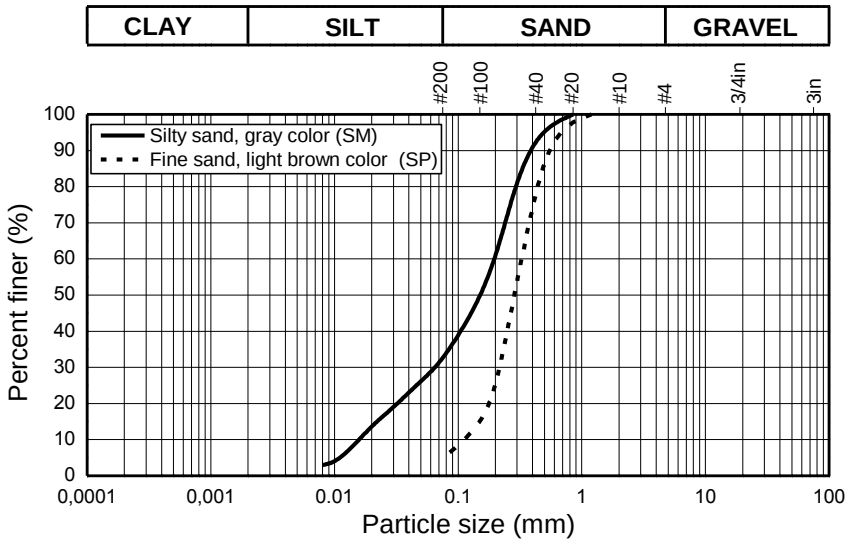

Figure 5. Grain size distribution of ejected materials from SITE-I.

Lateral spreading effects were observed on SITE-I involving ground fissures (up to about 200 m from the shore) with openings varying from 1 to 12 cm. Figure 6 depicts the location of the observed fissures and the vectors of accumulated displacements (estimated by summation of crack openings across a line perpendicular to the sea-shore). The overall lateral displacement on SITE-I is estimated at approximately 30 cm by summing the width of all crack openings along axis A-A΄, which is approximately perpendicular to sea-shore. It should be noted that no lateral spreading was observed in SITE-II.

According to an account by the landowner of SITE-I, in the late 1990's a part of the site (of unknown size and exact location) was excavated up to a depth of 4 m and the soil was replaced with un-compacted filling material of unknown composition. It is also worth mentioning that in the location indicated as "Overturned plastic water container" in Figure 2, the overturning in the east direction, of a 0.76 m tall, 0.5 m wide barrel-shaped plastic container filled with water, and resting on ground surface, was observed (Figure 7). According to the account of the land owner, the intensity of shaking was strong enough to make nearly impossible for people to stay on a standing position. This was confirmed by several witnesses (including 2 graduate students in Civil Engineering at U-Patras) that happened to be standing on the nearby beach at the time of the earthquake.

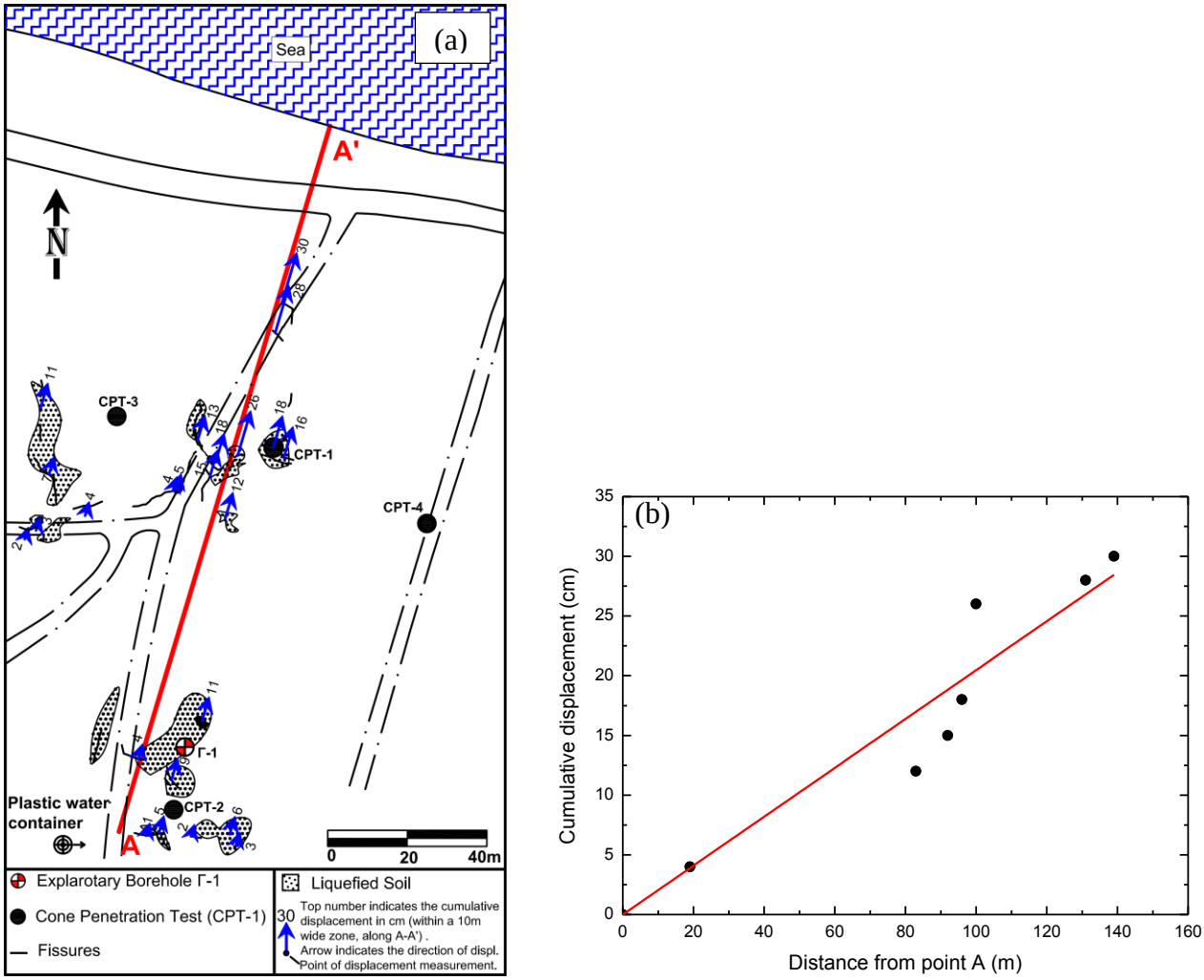

Figure 6. (a) Cumulative measured soil displacements in the coastal zone of Kato Achaia and (b) cumulative displacement vs distance along line AA'.

Figure 7. Barrel-shaped plastic water filled container which was overturned during the Achaia-Ilia 2008 earthquake.

GEOTECHNICAL INVESTIGATION

The subsurface investigation of the liquefied zone consisted of a combination of borings with sampling and SPT measurements, CPT measurements and in-situ evaluation of low-strain shear wave velocity by Surface Wave Methods: **S**pectral **A**nalysis of **S**urface **W**aves (SASW), **M**ulti-channel **A**nalysis of **S**urface **W**aves (MASW), **Re**fraction

Microtremor (ReMi), as shown in Figure 2 (Tran and Hiltunen, 2008, Pelekis and Athanasopoulos, 2011). Classification and shear strength laboratory tests were also conducted (Table 1). The actual delivered energy for each blow of the donut type hammer (operated with a cathead and rope system) was measured using an SPT Analyzer system (Figure 8). The results of the energy measurements show a mean energy ratio, ER (i.e. the ratio of measured impact energy to 100% of theoretical energy) of about 48%. Thus, the correction factor C_E, required in liquefaction triggering analyses, i.e. the ratio of impact energy to 60% of theoretical free-fall energy, is C_E=ER/60=0.8. It should be noted that the above value of C_E corresponds to the depth of formations susceptible to liquefaction (up to 12m depth in SITE-I) with no clear trend of C_E vs depth relation identified in the Kato Achaia site. To the extent of the authors knowledge this is the first time SPT energy measurements is conducted in Greece. All data obtained from the in-situ tests, and additional information, is available in digital form as accompanying files to this paper.

Results from this investigation are summarized in Figures 9 and 10. Figure 9 presents results for SITE-I, whose stratigraphy and soil properties can be represented by borehole G-1, cone penetration test CPT-2, and an average V_s-depth profile denoted as $V_{s\text{-}I}$. On the other hand, Figure 10 presents pertinent data for SITE-II, whose properties are represented by borehole G-2, cone penetration test CPT-5, and $V_{s\text{-}II}$. The values of low-strain shear wave velocity, V_s, in this study were measured by applying: 1) the SASW technique (utilizing APS-400 electromechanic vibrators and a pair of Wilcoxon 1 Hz vertical seismic accelerometers), 2) the MASW technique (utilizing 12 vertical 4.5 Hz geophones and an impact source of energy), and 3) the ReMi technique (utilizing ambient microtremor recorded by 12 vertical 4.5 Hz geophones). Several surface wave measurements were performed at each of the two sites, as shown in Figure 2. At each site the variation between different methods of measurement was insignificant, thus an average V_s-depth profile was derived, based on all measurement methods and locations, denoted as $V_{s\text{-}I}$ and $V_{s\text{-}II}$, for SITE-I and SITE-II, respectively.

It is observed that the soil profiles in SITE-I and SITE-II (Figures 9 and 10) exhibit similarities, but also noticeable differences. Indeed, in both sites the stratigraphy involves a surface layer of coarse-grained material (sandy gravel) with a small amount of fines, followed by a layer of cohesive material of medium plasticity and low strength. The thickness of surface zone is different in two sites: about 12 m in SITE-I (including some non-plastic sand/silt layers with low fines content) and 4 m in SITE-II. These layers are underlain by low-strength cohesive materials with large fines content. On SITE-II, fine grained formations (FC up to 90%, PI = 7 to 18) are encountered below 4 m whereas similar formations are encountered below 12 m in SITE-I. Results from SPT and CPT tests indicate that the strength of deep formations in SITE-I is greater than corresponding strengths in SITE-II [$(N_1)_{60} \approx 20$ vs. 9 and $q_c \approx 0.9$ MPa vs. 0.6 MPa]. On the other hand, low-strain shear wave velocities, V_s, do not exhibit significant differences in the two sites, being equal to approximately 150 m/s in both profiles. Note that water table elevation in the area at the time of the tests (February 2009) was located 0.4 m below the ground surface.

Figure 8. Field energy ratio measurements during SPT testing. (SPT Analyzer, Pile Dynamincs Inc.)

Table 1. Results of borehole geotechnical investigation at SITE-I and SITE-II.

	Borehole number	Sample number	Sample depth	Classification USCS	Grain size distribution					Coefficient of uniformity, C_u	Water content, w (%)	Atterberg limits			Total weight		Unconfined compression strength, q_u (kPa)
					Gravels	Sand	Fines	Silt	Clay			LL (%)	PL (%)	PI (%)	γ_{wet} (kN/m^3)	γ_{dry} (kN/m^3)	
SITE-I	G-1	#1	1.80-2.00	GM	39	38	23	19	4	333	10.09	N.P.			-	-	-
	G-1	#2	2.80-3.00	SM	15	63	22	18	4	63	-	N.P.			-	-	-
	G-1	#3	3.85-4.00	SP	16	80	4	4	-	6	-	N.P.			-	-	-
	G-1	#4	4.80-5.00	GW	49	46	9	9	-	6	-	N.P.			-	-	-
	G-1	#5	5.50-6.00	ML	1	30	69	57	12	35	-	N.P.			-	-	-
	G-1	#6	6.45-6.80	SM	26	41	33		9	150	-	N.P.			-	-	-
	G-1	#7	7.30-7.50	SM	2	67	31	24	7	46	-	N.P.			-	-	-
	G-1	#8	9.00-12.00	SP	4	93	3	3	-	3	-	N.P.			-	-	-
	G-1	#9	12.00-12.30	-	-	-	-	-	-	-	26.77	41	22	19	19.29	15.22	122
	G-1	#10	12.70-13.00	CL	-	5	95	59	36	-	30.08	39	22	17	18.74	14.41	92
	G-1	#11	13.40-13.70	CL	-	12	88	61	27	-	28.94	35	22	13	19.68	15.26	83
	G-1	#12	14.50-14.70	SM	1	55	44	33	11	64	-	N.P.			-	-	-
	G-1	#13	16.00-16.50	CL	-	3	97	40	57	-	33.36	47	26	21	19.88	14.91	71
	G-1	#14	17.30-17.70	ML	-	6	94	55	39	-	38.8	40	28	12	19.35	13.94	94
	G-1	#15	18.50-19.00	ML	-	8	92	60	32	-	31.18	40	28	12	19.14	14.59	96
SITE-II	G-2	#16	1.00-1.20	SW	37	58	5	5	-	21	-	N.P.			-	-	-
	G-2	#17	2.45-2.80	GP-GM	47	46	7	7	-	54	-	N.P.			-	-	-
	G-2	#18	3.50-3.80	SP	10	85	5	5	-	6	-	N.P.			-	-	-
	G-2	#19	4.00-4.60	ML	-	33	67	55	12	47	-	N.P.			-	-	-
	G-2	#20	4.70-4.90	ML	-	6	94	59	35	-	36.7	40	27	13		-	31
	G-2	#21	5.00-5.50	CL	-	4	96	55	41	-	38.79	43	25	18	19.69	14.19	48
	G-2	#22	7.00-7.30	ML	-	12	88	60	28	-	29.97	37	25	12	18.34	14.11	71
	G-2	#23	7.30-7.50	OL	-	9	91	60	31	-	43.36	37	25	12	18.69	13.04	85
	G-2	#24	8.50-9.00	ML	-	16	84	61	23	-	28.56	31	24	7	19.34	15.04	75
	G-2	#25	9.50-9.80	OL	-	5	95	55	40	-	32.15	40	27	13	19.84	15.01	84
	G-2	#26	9.80-10.00	SP-SM	-	92	7	3	4	22	-	N.P.			-	-	-
	G-2	#27	10.45-10.65	CL	-	7	93	50	43	-	33.43	35	24	11	19.65	14.73	73
	G-2	#28	14.70-15.00	ML	-	1	99	62	37	-	29.39	39	26	13	19.18	14.82	45
	G-2	#29	16.30-16.50	-	-	-	-	-	-	-	29.63	-	-	-	20.05	15.47	65
	G-2	#30	16.70-17.00	CL	-	10	90	52	38	-	27.37	34	23	11	19.79	15.54	64
	G-2	#31	19.00-19.40	CL	-	10	90	59	31	-	24.89	34	23	11	19.43	15.56	113
	G-2	#32	21.30-21.70	CL	-	6	94	58	36	-	32.56	41	25	16	18.88	14.24	74
	G-2	#33	23.60-24.00	CL	-	7	93	54	39	-	31.73	41	25	16	19.18	14.56	95

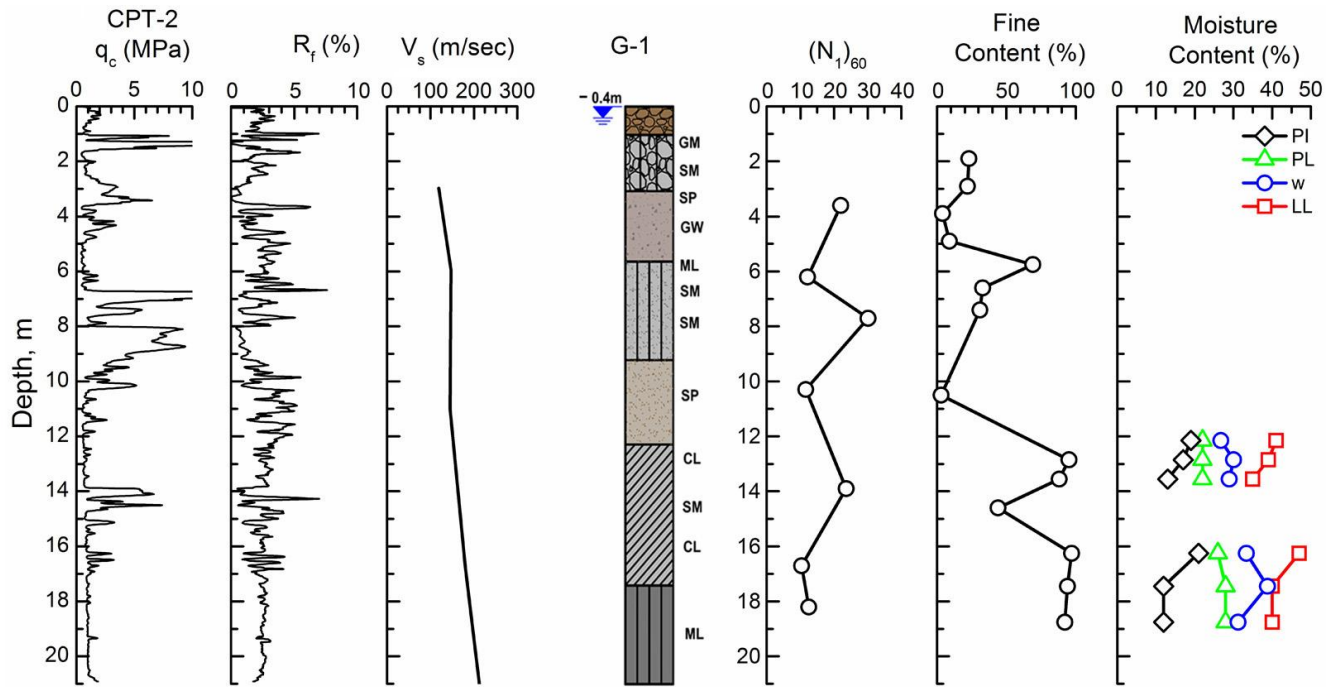

Figure 9. Summary of results of subsurface exploration at SITE-I.

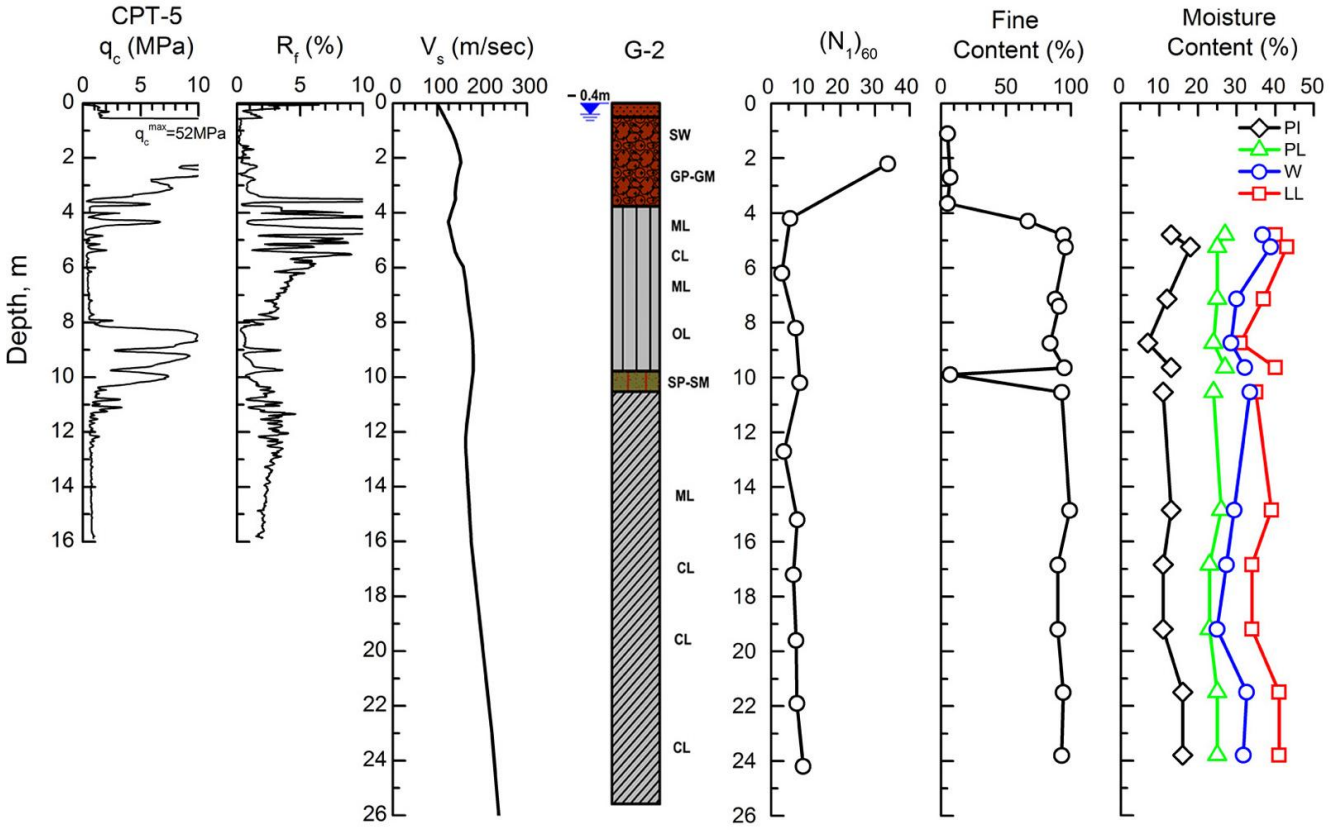

Figure 10. Summary of results of subsurface exploration at SITE-II.

In the present study the availability of measured values of N_{SPT}, q_c and V_s at nearby locations in SITE-I and SITE-II, provides an opportunity to check a number of empirical correlations, proposed by several investigators. The graph in Figure 11 compares measured values of N_{SPT} with those predicted by available V_s- N_{SPT} correlations. It is observed that in SITE-II the Athanasopoulos (1995) and Hasancebi and Ulusay (2006) predictions are in good agreement with the measured values. On the contrary, in SITE-I a disagreement is observed between measured and predicted values, which may be due to biased N_{SPT} measurements caused by the presence of gravels. Another interesting comparison is depicted in Figure 12, where measured values of q_c are compared to predictions based on SPT-CPT correlations. It is observed that for SITE II the agreement is indeed very good, whereas for SITE-I, significant deviations exist from 4 to 6 m and 11 to 14 m. This discrepancy, again suggests that the SPT blow count may have been affected by the presence of gravels. Finally, a comparison between measured values of V_s and estimates based on CPT soundings is shown in Figure 13. In this case, the agreement is better for both sites – compared to N_{SPT} correlations – indicating the greater potential of q_c-V_s correlations for estimating reliable V_s values from CPT results (in the particular area of SITE-I and SITE-II).

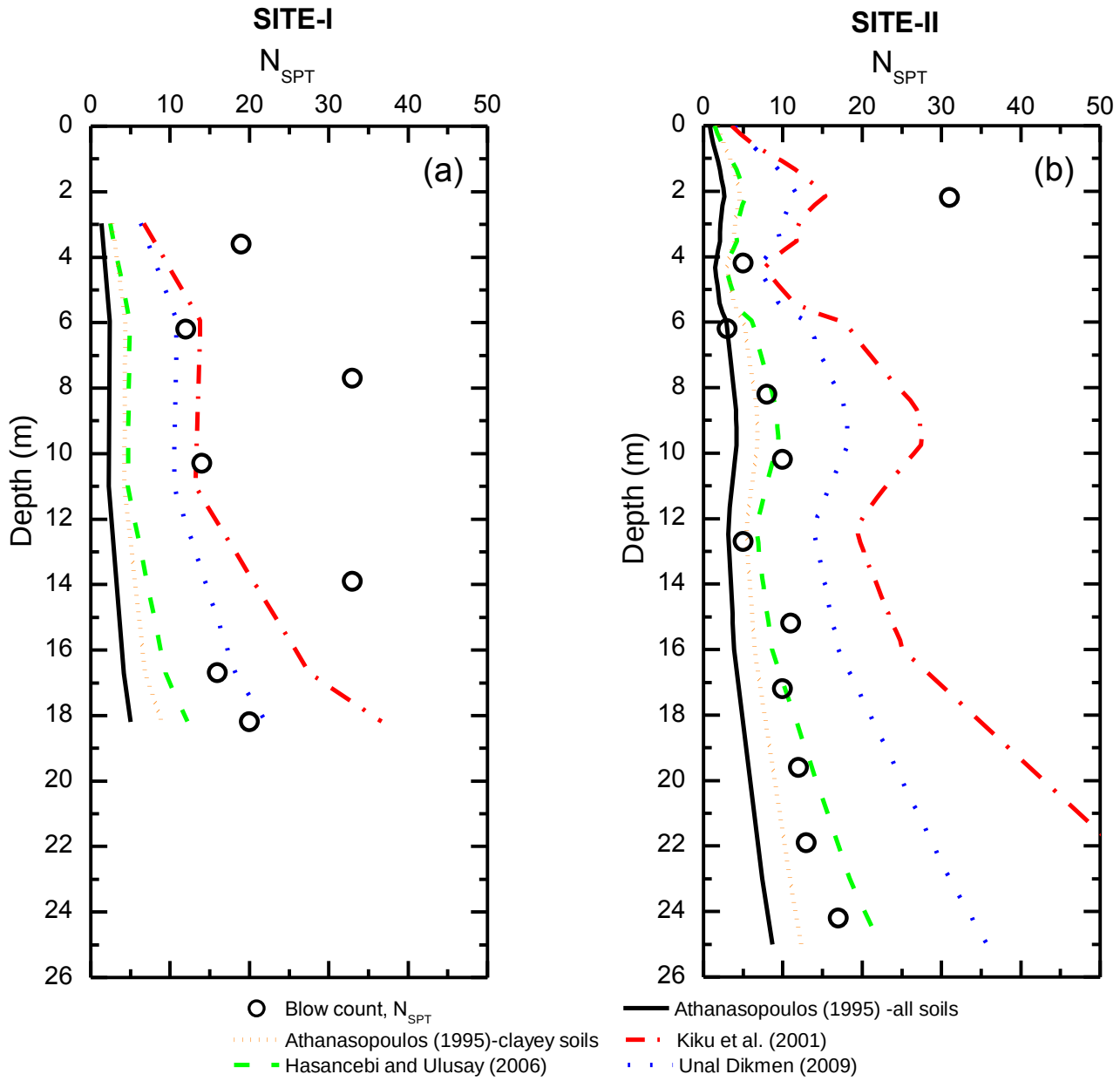

Figure 11. Comparison between measured N_{SPT} blow count and corresponding values predicted using V_s-N_{SPT} correlations.

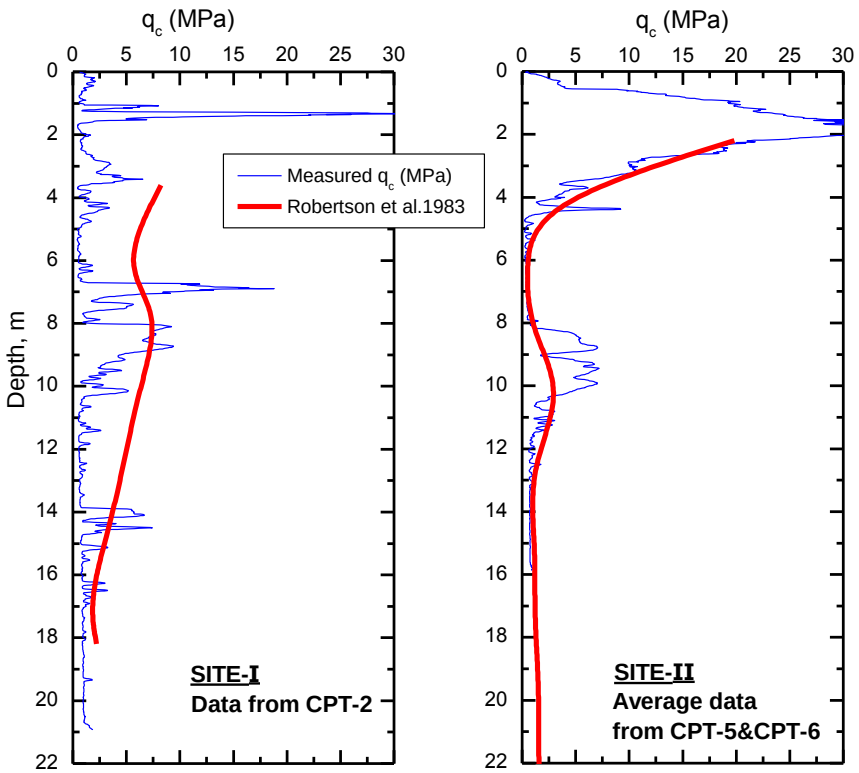

Figure 12. Comparison between measured CPT values and values predicted using the Robertson et al. (1983) SPT-CPT correlation .

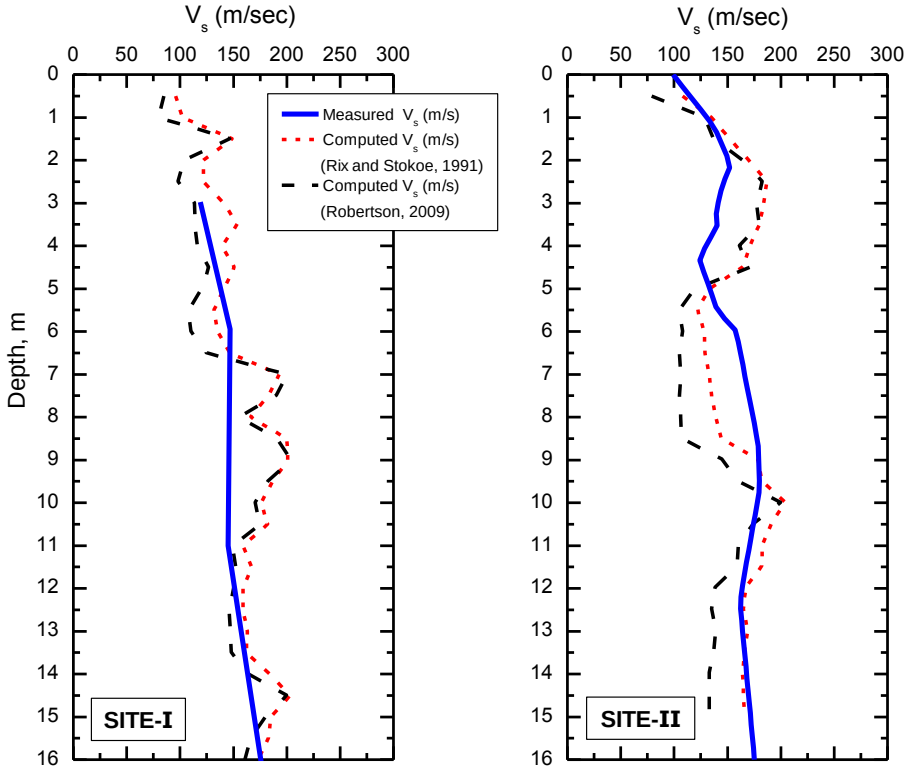

Figure 13. Comparison between measured shear wave velocity V_s(m/s) and values predicted using the Rix and Stokoe, (1991) and Robertson (2009) CPT-V_s correlations .

GROUND MOTION AT THE LIQUEFACTION SITE

Despite the fact that the Achaia-Ilia (2008) earthquake was recorded by 27 strong motion instruments (Margaris et al., 2008), no strong motion recording of the main shock was obtained in the vicinity of the liquefied coastal site being examined in the present study. Therefore, an estimate of peak horizontal acceleration in the greater area of Kato Achaia, caused by the Achaia-Ilia 8 June 2008 earthquake, can be obtained 1) based on applying the NGA attenuation relation of Boore and Atkinson 2008 (Figure 14) utilizing a suite of 18 acceleration time histories of the main event, recorded between 15 and 100 km from causative fault (Margaris et al 2008, 2010) and 2) based on the shakemap (Figure 15) reported by the USGS (http://earthquake.usgs.gov/earthquakes/shakemap/global/shake/2008taaw/). The application of the above two approaches gives similar results for the mean value of peak ground acceleration at the location of Kato Achaia: 0.33g from the above attenuation relationship and 0.37g from the shakemap. The uncertainty associated with the mean values of PGA according to the aforementioned USGS shakemap is shown to be below 0.5%g.

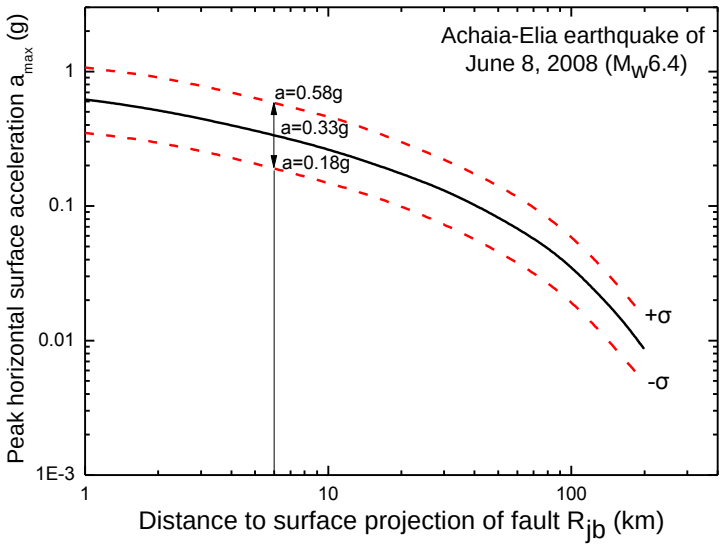

Figure 14. Boore and Atkinson (2008) attenuation of maximum horizontal surface acceleration with distance R_{jb} from fault; the particular attenuation relationship is in good aggreement with the recorded surface accelerations in the M_w 6.4 Achaia-Ilia 2008 earthquake (Margaris et al., 2010).

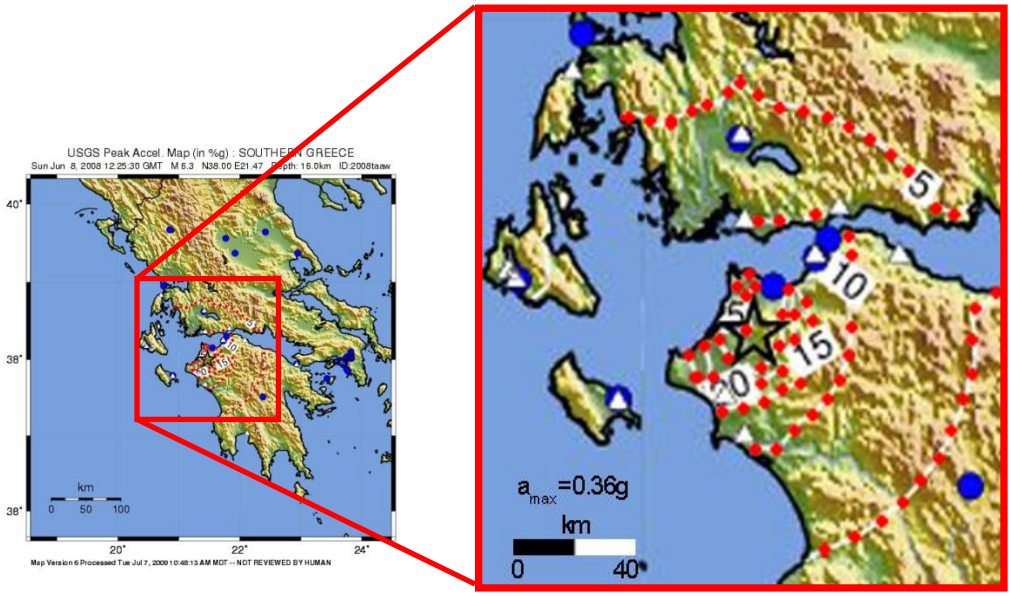

Figure 15. Shakemap for the 8 June 2008 event by USGS (http://earthquake.usgs.gov/earthquakes/shakemap/global/shake/2008taaw/).

It should be anticipated, however, that the above values of PGA (0.33g to 0.37g) actually reflect the response at the elevated part of the town, far from the coast line area where local site effects are expected to have played a decisive role in modifying the surface motion. In this respect, the back analysis of observed behavior of the overturned plastic container during the main shock (Figure 7) could provide valuable information regarding the lower bound of surface acceleration developed in the vicinity of liquefaction site. The location of the plastic container is shown in Figure 2 and Figure 6 and, based on the account of the land owner, it was full of water and uncovered, at the time of the main shock. It is known that the behavior of rigid blocks under pulse (or earthquake) shaking depends on shaking intensity, frequency content, slenderness and base conditions (Mylonakis, 2013). In particular, the frequency content of excitation is an important parameter that plays a decisive role in the overturning of the container. Pertinent studies have shown that the acceleration value required to overturn a rigid body increases with decreasing frequency, f, (or increasing period, T) values and reaches the highest value for the pseudostatic case (i.e. f=0Hz or T=∞) which corresponds to the simple solution a_g=(B/H)g. In the case of water-filled, uncovered container the behavior is further complicated by the response of the mass of water, and to the best of authors' knowledge, no analytical solution is available in the literature. Therefore, in the present study it was decided to seek an experimental solution to the problem by utilizing the shaking table facility of the Department of Civil Engineering of the University of Patras.

In the shaking table tests performed in this study, the original overturned plastic container was used, filled with water, and resting on either an Expanded Polystyrene (EPS15) foundation mat or on a silty sand layer. The critical acceleration required for overturning the container was identified as accurately as possible by increasing the intensity of shaking in very small increments (0.02g) to identify with certainty the lower bound value of PGA, and by using a time history of shaking that resembled, as closely as possible, the actual motion of the coastal area (in terms of frequency content). The shaking tests of the water filled container were performed outside the shaking table, using the mechanism shown in Figure 16, to avoid water entering into the shaking table installations. In the shaking table tests the uni-directional horizontal time history (shown in Figure 17c) was used as input motion. This time history was derived by utilizing the acceleration record (PGA=0.125g) of the Patra (kiosk) accelerograph station, located at R_{jb}=16.7 km from the causative fault (Margaris et al., 2010). This motion was transferred to liquefaction sites of Kato Achaia at a distance of R_{jb}=6 km from the causative fault, using Boore and Atkinson (2008) attenuation relation. Using the above procedure the time history shown in Figure 17c was derived, which is characterized by the Fourier spectrum (with a predominant period T≈1 sec) shown in Figure 17d. In order to identify the peak ground acceleration required to overturn the plastic container, a number of shaking table tests was performed, using the motion shown in Figure 17c (Patra-kiosk) scaled to peak values ranging from 0.10 to 0.22g.

The results of testing indicated that the plastic container was overturned at a_{max} ranging from 0.17 (averaging the values of 0.15g and 0.18g shown in Figure 17c) to 0.20g (averaging the values of 0.19g and 0.21g shown in Figure 17c), depending on the sitting conditions of the container (soil layer in Figure 17b and EPS15 block in Figure 17a). Considering the results of the above two approaches the lower bound peak ground acceleration at the liquefaction sites can be taken to be equal to a_{max}≈0.18g, with a possible range of variation from 0.17g to 0.20g.

An upper bound PGA value at the coastal zone of Kato Achaia (for the main event of 2008 Achaia-Ilia earthquake) has been derived by the authors in a separate study (presently under preparation for submission) focusing on topographic amplification of motion at the elevated part of the town. This particular study was based on 2D/1D finite element site response analyses and the type and extent of observed damage at the elevated part of the town. The above analyses have indicated that the value of surface acceleration at the coastal zone of Kato Achaia (during the main shock) must have been approximately equal to 0.2g. Interestingly, this calculated value of horizontal acceleration of the coastal zone coincides with the upper limit of threshold acceleration range identified from the shaking table tests of the present study. Therefore, based on the above findings, it was concluded that the PGA value developed at the liquefaction site of Kato Achaia can be taken to be equal to a_{max}≈0.18g.

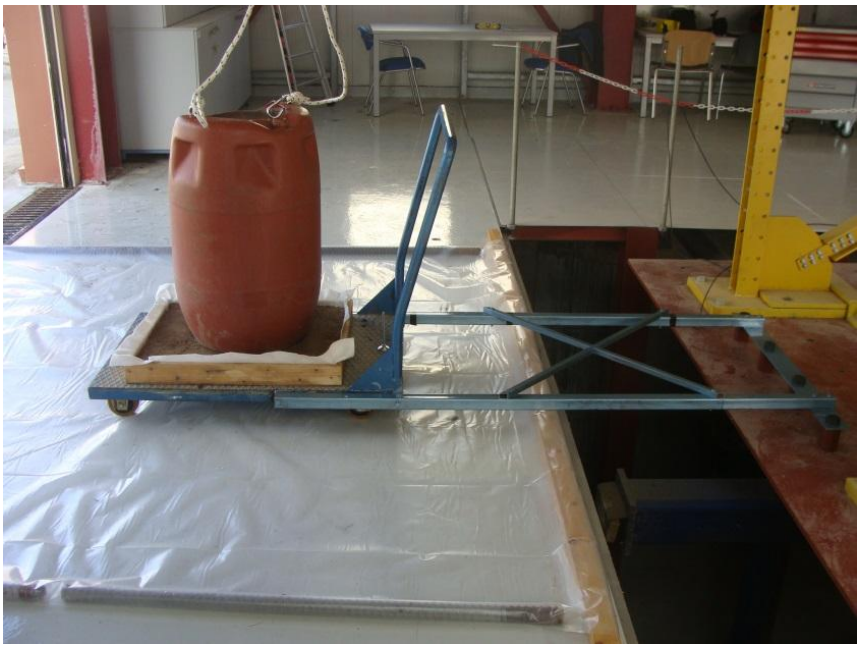

Figure 16. Mechanism used for performing shaking tests on the water filled plastic container by utilizing the University of Patras Shaking Table facility.

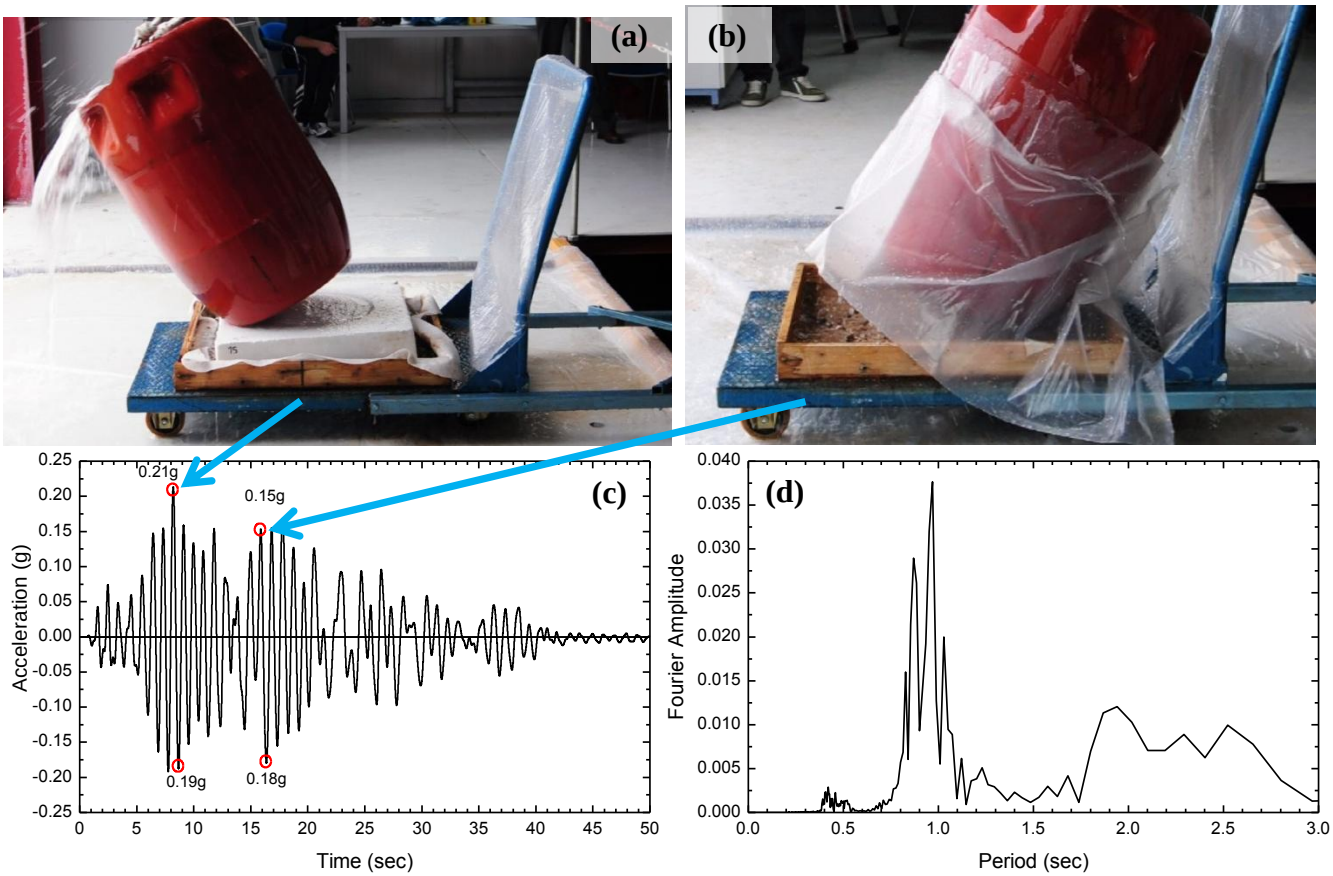

Figure 17. Results of shaking table tests on the plastic barrel-shaped container, filled with water (a) overturning of container sitting on EPS15 block, under a_{max}≈0.20g, (b) overturning of container sitting on silty sand layer, under a_{max}≈0.17g, (c) scaled acceleration time history (recorded at Patra-kiosk) used as input in the shaking table tests and (d) Fourier Spectrum of input motion.

PREDICTED VS. OBSERVED FIELD PERFORMANCE

The objective of the current study – as stated in the introduction – is the presentation of detailed geotechnical and earthquake shaking data, along with descriptions of field performance in the case of Achaia-Ilia M_w 6.4 earthquake with the intend to generate a well-documented liquefaction case history upon which further liquefaction analyses could be based in the future. For the sake of completeness of the present work, however, a brief comparison of the observed performance to that predicted by currently available liquefaction triggering charts is included in this section.

At present, the most widely used liquefaction triggering charts are based on in-situ testing results, namely, (a) the blow count, N_{SPT}, of the standard penetration test (SPT) (Cetin et al. 2004, Idriss and Boulanger 2008, Seed 2010), (b) the tip resistance, q_c , of cone penetration test (CPT) (Moss et al. 2006, Idriss and Boulanger 2008), and (c) the value of low-amplitude shear wave velocity, V_s (Andrus and Stokoe 2000, Youd et al., 2001, Idriss and Boulanger 2008). It should be noted that Kayen et al. (2013) have recently developed a probabilistic liquefaction triggering chart (in terms of the corrected value of shear wave velocity V_{s1}) which will not be included in the comparisons performed in this section. As was mentioned, the SPT measurements reported in the present study are likely affected by a significant amount of large size gravels encountered in the borehole. For this reason, the comparisons presented are limited to only CPT and V_s measurements.

In the diagrams of Fig. 18, all data points generated in the present study for sand-like materials (in terms of corrected / normalized q_c values and cyclic stress ratios CSR) for SITE I and SITE II are superposed to the Idriss and Boulanger (2008) deterministic liquefaction triggering chart (which, for q_{c1Ncs}<100, does not deviate significantly from the Moss et al., 2006 probabilistic chart). The comparison indicates that the development of liquefaction is clearly predicted for SITE I (with only point #7 being marginal). On the other hand, the points corresponding to SITE II are either close to the boundary line or entirely outside the liquefaction area of the diagram, indicating marginal or no liquefaction. Similarly, in the diagrams of Fig. 19, depicting in a deterministic way the liquefaction triggering potential in terms of the corrected value of shear wave velocity V_{s1} (Youd et al., 2001), all data points for SITE I are located in the liquefaction triggering area of the diagrams, whereas for SITE II, the corresponding data points, either fall in the vicinity of the boundary line or outside the liquefaction area of the diagram. It may therefore be concluded that the currently available liquefaction triggering charts, in terms of in-situ CPT and V_s data, have successfully predicted the observed field performance for the liquefied coastal zone of Kato Achaia.

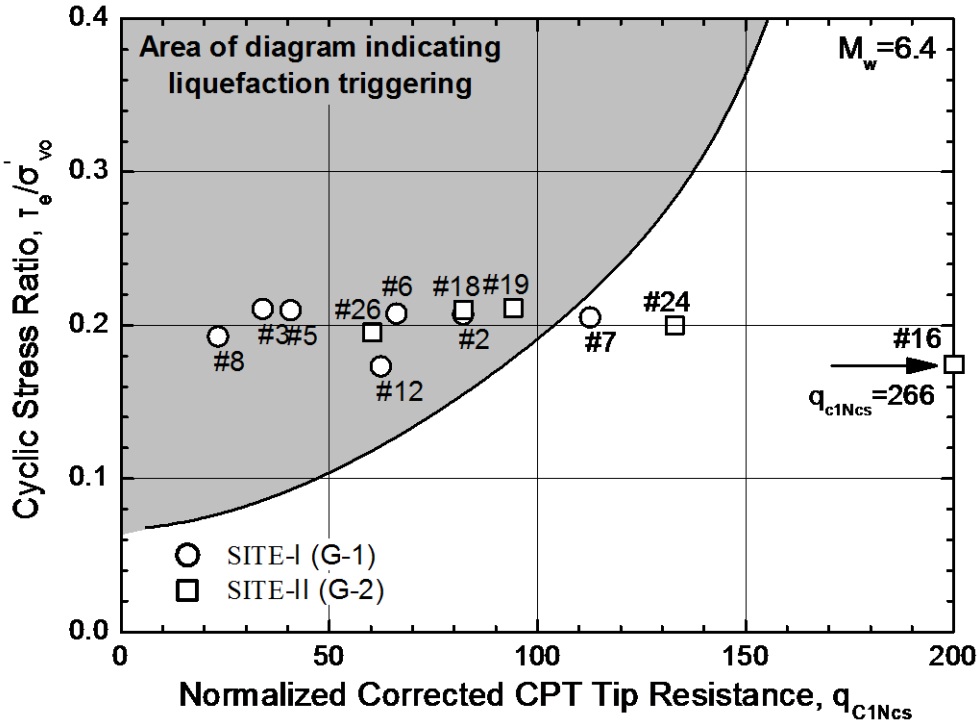

Figure 18. Liquefaction triggering chart based on CPT tip resistance q_{c1Ncs}, with data points from the case history presented in this paper.

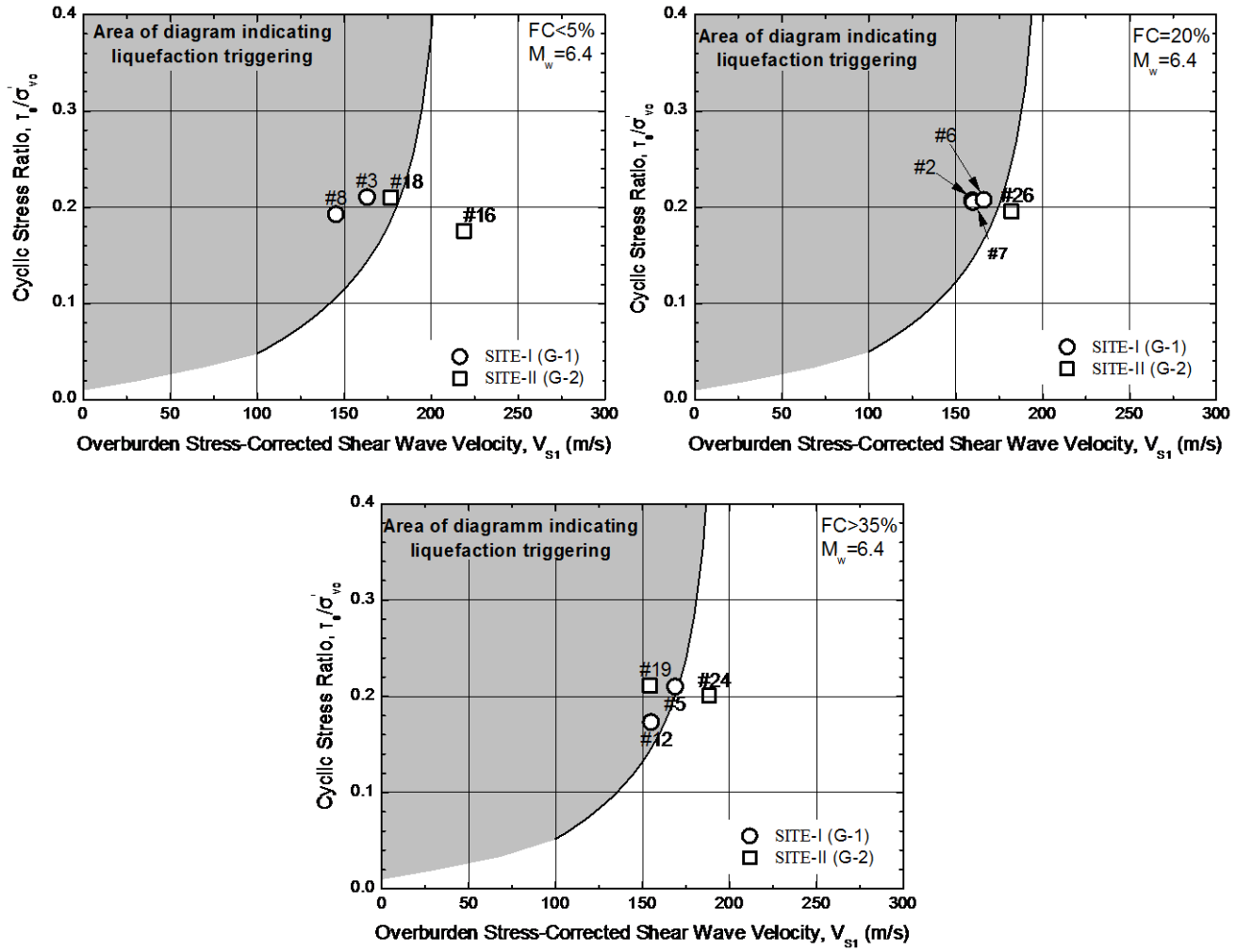

Figure 19. Liquefaction triggering charts based on shear wave velocity V_{S1}, with data points from the case history presented in this paper.

CONCLUSIONS

During the reconnaissance effort in the coastal zone of Kato Achaia following the June 8, 2008 M_w 6.4 earthquake, cases of extensive soil liquefaction (accompanied by lateral spreading), marginal liquefaction, and nonliquefaction were detected. These observations were followed by 1) a detailed in-situ and laboratory soil investigation involving SPT, CPT and Surface Wave velocity measurements, conducted by the authors and other team members, and 2) an assessment of the peak ground acceleration at the liquefaction area based on the results of shaking table tests on a plastic water container, which was sitting on the ground at a nearby location and was overturned in the June 8, earthquake. The main findings of the above effort can be summarized as follows:

1. Soil liquefaction was observed at two sites of the coastal zone: At SITE-I the phenomenon was extensive and was accompanied by soil fissuring and lateral spreading (~0.30 m) towards the sea shore. An exploratory borehole (G-1) was drilled in this site (at the location of soil ejecta) up to a depth of 20.5 m, with SPT measurements and soil sampling. Three CPT soundings were also performed in this site, in the vicinity of the observed sand craters. An additional CPT sounding was also performed at a location outside the liquefied area, where no signs of ground failure were observed. Finally, surface wave measurements (MASW, SASW, ReMi) were conducted in the liquefied area and Vs-depth profiles were established up to a depth of 16 to 20 m, from ground surface. At SITE-II (at distance of ~350 m from SITE-I) only marginal liquefaction or nonliquefaction was observed, with no signs of lateral spreading (or soil fissures). In this site an exploratory borehole (G-2) with SPT measurements and soil

sampling was drilled up to a depth of ~24m. CPT soundings were also conducted, to a depth of 16 m as well as surface measurements at four nonliquefaction locations.

2. A detailed soil investigation was performed at the two liquefaction sites (SITE-I and SITE-II), which included in-situ (SPT, CPT, SASW, MASW, ReMi) and laboratory (classification, strength) testing to characterize the soil formations at the two sites. The investigation showed a general similarity of conditions at the two sites with the following differentiations: 1) the thickness of liquefiable sand-silty sand layers in SITE-I is much larger than in SITE-II, which suggests that greater amount of ejecta would be expected in earthquake shaking in SITE-I compared to SITE-II, 2) the existence of larger amount of gravels in SITE-I (from 4 to 12 m) may have affected the NSPT values in this depth zone, making them less reliable for liquefaction triggering predictions. Finally, the small amplitude shear above velocity, Vs, vs depth profiles at two sites, show only minor differentiation and may be assumed that a single Vs-depth profile represents the conditions at both sites (SITE-I and SITE-II).
3. An assessment of peak ground acceleration at the liquefied/nonliquefied locations was based on (a) shaking table simulation of the behavior of an overturned plastic, barrel-shaped container which, during the main shock, was sitting (filled with water) on the ground surface in the liquefaction area and (b) the results of a separate study on topographic amplification at the elevated part of Kato Achaia. Based on the results of shaking table tests and of numerical response analyses, it was concluded that the ground acceleration at the coastal zone of Kato Achaia (during the main shock of the Achaia-Ilia (Greece) Mw 6.4, 2008 earthquake) can be taken to be equal to amax≈0.18g.
4. The data presented herein, can be used (a) for checking the validity of current liquefaction susceptibility criteria and liquefaction triggering relationships (for this particular shallow crustal earthquake), and (b) for establishing a well-documented liquefaction case history, which could augment the worldwide data bases in terms of SPT, CPT and Vs data.
5. Results of preliminary comparisons indicate that currently available CPT– and Vs–based liquefaction triggering charts, successfully predicted the field performance of the Kato Achaia coastal zone in the 2008 Achaia-Ilia Mw 6.4 earthquake.

ACKNOWLEDGMENTS

The authors thank Prof. N. Klimis, Prof. J. Stewart, Prof. G. Mylonakis and V. Efthymiadou, M.Sc, for their help during the Kato Achaia reconnaisance effort, Dr. P. Kloukinas, and E. Pefani, M.Sc, for participating in the soil characterization tests, and Dr. P. Psimoulis and doctoral student S. Likourgiotis for surveying the liquefied area at SITE-I. The authors are also indebted to Assoc. Professor P. Bousias, and Post doc researcher Dr. E. Strepelias, Structures Laboratory, Dept. of Civil Engineering, University of Patras, for their help in the shaking table tests of the present study.

REFERENCES

Andrus, R. D. and Stokoe K. H., II. (2000). "Liquefaction Resistance of Soils from Shear-Wave Velocity", Journal of Geotechnical and Geoenvironmental Engineering, ASCE, November 2000, Vol. 126, No. 11, 1015-1025.

Athanasopoulos, G.A. (1995). "Empirical Correlations V_{so}-N_{SPT} for Soils of Greece: A Comparative Study of Reliability", Transactions the Wessex Institute, www.witpress.com, Paper DOI: 10.2495/SD950031, Proc. of Seventh International Conference on Soil Dynamics and Earthquake Engineering, Chania, Greece, (Eds. A.S. Cakmak and C.A. Brebbia), 19-26.

Batilas, A., Pelekis, P., Vlachackis, V., Athanasopoulos, G., Mylonakis, G. (2008). "Soil liquefaction in the Achaia-Elia, Greece, earthquake– field evidence, simplified analyses and EC-8 provisions", Proceedings of ERTC-12 Workshop on evaluation of EC-8, XV European Conference on Soil Mechanics & Geotechnical Engineering, Athens, September 11, 2011.

Boulanger, R. W., and Idriss, I. M. (2012). "Examination and Reevalaution of SPT-Based Liquefaction Triggering Case Histories", Journal of Geotechnical and Geoenvironmental Engineering, ASCE, 138(8), 898-909.

Caputo, R. and Papathanassiou, G. (2012). "Ground failure and liquefaction phenomena triggered by the 20 May 2012 Emilia-Romanga (Northern Italy) earthquake case study of Sant'Agostino-San Carlo-Mirabello zone", Natural Hazards and Earth System Sciences, 12, 3177-3180.

Cetin, K. O., Seed, R. B., Der Kiureghian, A., Tokimatsu, K., Harder, L. F., Kayen, R. E., and Moss, R. E. S. (2004). "Standard penetration test-based probabilistic and deterministic assessment of seismic soil liquefaction potential." Journal of Geotechnical and Geoenvironmental Engineering, ASCE, Vol. 130(12), 1314–1340.

Cubrinovski, M., Bray, I.D., Taylor, M., Giorgini, S., Bradley, B., Wotherspoon, L., and Zupan, I., (2011). "Soil Liquefaction effects in the Central Business District during the February 2011 Christchurch earthquake", Seismological Research Letters, 82(6), 893-904.

GEER (2010). "Geotechnical Reconnaissance of the 2010 Darfield (New Zealand) Earthquake", Version 1: 14 November 2010.

GEER (2010). "Geo-Engineering Reconnaissance of the February 27, 2010 Maule, Chile Earthquake", Version 2: 25 May 2010.

GEER (2010). "Geotechnical Engineering Reconnaissance of the 2010 Haiti Earthquake", Version 1: 22 February 2010.

GEER (2011). "Geotechnical Reconnaissance of the 2011 Christchurch, New Zealand Earthquake", Version 1: 15 August 2011.

Hasancebi, N., and Ulusay, R. (2006). "Empirical correlations between shear wave velocity and penetration resistance for ground shaking assessments", Bull. Eng. Geol. Environ., 66, 203–213.

Idriss, I.M. and Boulanger, R.W. (2008). "Soil Liquefaction during Earthquakes", Earthquake Engineering Research Institute MNO-12, 242.

Ishihara, K. (2012). "Liquefaction in Tokyo Bay and Kanto Regions in the 2011 Great East Japan Earthquake", Proceedings of the International Symposium on Engineering Lessons Learned from the 2011 Great East Japan Earthquake, March 1-4, 2012, Tokyo, Japan, 63-81.

Kayen, R., Moss, R.E.S., Thompson, E.M., Seed, R.B., Cetin, K.O., Der Kiureghian, A., Tanaka, Y. and Tokimatsu, K. (2013). "Shear-Wave Velocity-Based Probabilistic and Deterministic Assessment of Seismic Soil Liquefaction Potential" Journal of Geotechnical and Geoenvironmental Engineering, ASCE, Vol. 139(3), 407–419.

Kiku, H., Yoshida, N., Yasuda, S., Irisawa, T., Nakazawa, H., Shimizu, Y., Ansal, A., and Erkan, A. (2001). "In-situ penetration tests and soil profiling in Adapazarı, Turkey", Proc. ICSMGE/TC4 Satellite Conf. on Lessons Learned from Recent Strong Earthquakes, 259–265.

Lai, C.G., Bozzoni, F., Mangriotis, M-D. and Martinelli, M. (2012). "Geotechnical Aspects of May 20, 2012 M5.1 Emilia Earthquake, Italy", EUCENTRE, July 2012.

Margaris, B. and 18 other authors (2008). "Preliminary Report on the Principal Seismological and Engineering Aspects of the Mw=6.5 Achaia-Ilia (Greece) Earthquake on 8 June 2008". GEER Association Report No. GEER-013, June 2008, http://www.geerassociation.org/GEER_Post%20EQ%20Reports/Greece_2008/Cover_Greece2008.html.

Margaris, B., Athanasopoulos, G., Mylonakis, G., Papaioannou, C., Klimis, N., Theodoulidis, N., Savvaidis, A., Efthymiadou, V. and Stewart, J. (2010). "The 8 June 2008 M_w6.4 Achaia-Ilia, Greece Earthquake: Source Characteristics, Ground Motions, and Ground Failure", Earthquake Spectra, 26(2), 399-424.

Moss, R. E. S., Seed, R. B., Kayen, R. E., Stewart, J. P., Der Kiureghian, A., and Cetin, K. O. (2006). "CPT-Based Probabilistic And Deterministic Assessment Of In Situ Seismic Soil Liquefaction Potential." Journal of Geotechnical and Geoenvironmental Engineering, ASCE, Vol. 132(8), pp. 1032–1051.

Moss R.E.S., Kayen, R.E., Tong, L.-Y., Liu, S.-Y., Cai, G.-J., and Wu, J. (2011). "Retesting of Liquefaction and Nonliquefaction Case Histories from the 1976 Tangshan Earthquake", Journal of Geotechnical and Geoenvironmental Engineering, ASCE, 137(4), 334-343.

Mylonakis, G. (2013). Personal communication.

Orense R.P., Pender, M.J., and Wotherspoon, L.M. (2012). "Analysis of Soil Liquefaction during the recent Canterbury (New Zealand) Earthquakes", Geotechnical Engineering Journal of the SEAGS & AGSSEA, June, 2012, 43(2), 8-17.

Pelekis, P.C. and Athanasopoulos, G.A., (2011). "An Overview of Surface Wave Methods and a Reliability Study of a New Simplified Inversion Technique", Soil Dynamics and Earthquake Engineering, 31(12), 1654-1668.

Rix, G.J., and Stokoe, K.H. (1991). "Correlation of Initial Tangent Modulus and Cone Penetration Resistance", International Symposium on Calibration Chamber Testing. In Proceedings of ISOCCT-1, ed. A. B. Huang,. Elsevier Publishing, New York, 351-362.

Robertson, P.K. (2009). "Interpretation of Cone Penetration Tests –a unified approach," Canadian Geotechnical Journal, 46(11), 1337-1355.

Robertson, P.K., Campanella, R.G., and Wightman, A. (1983). "SPT-CPT Correlations", Journal of Geotechnical Engineering, 109(11), 1449-1459.

Seed, R.B. (2010). "Technical Review and Comments: 2008 EERI Monograph "Soil Liquefaction During Earthquakes (by I.M. Idriss and R.W. Boulanger)", Geotechnical Report No. UCB/GT-2010/01, University of California at Berkeley, 75.

Tran, K.T. and Hiltunen, D.R. (2008). "A Comparison of Shear Wave Velocity Profiles from SASW, MASW, and ReMi Techniques", Geotechnical Earthquake Engineering and Soils Dynamics IV, Sacramento, CA, USA, 18-22 May, 2008, ASCE, GSP 181.

Tsukamoto, Y., Kawabe, S., and Kokusho, T. (2012). "Soil liquefaction observed at the lower stream of Tonegawa river during the 2011 off the Pacific Coast of Tohoku Earthquake", Soils and Foundations, 52(5), 987-999.

Verdugo, R. (2012). "Comparing Liquefaction Phenomena Observed during the 2010 Maule, Chile, Earthquake and 2011 Great East Japan Earthquake", Proceedings of the International Symposium on Engineering Lessons Learned from the 2011 Great East Japan Earthquake, March 1-4, 2012, Tokyo, Japan, 707-718.

Yamaguchi, A., Mori, T., Kazama, M., and Yoshida, N. (2012). "Liquefaction in Tohoku district during the 2011 off the Pacific Coast of Tohoku Earthquake", Soils and Foundations, 52(5), 811-829.

Yasuda, S., Harada, K., Ishikawa, K., and Kanemaru, Y. (2012). "Characteristics of liquefaction in Tokyo Bay area by the 2011 Great East Japan earthquake", Soils and Foundations, 52(5), 793-810.

Youd, T. L., Idriss, I. M., Andrus, R. D., Arango, I., Castro, G, Christian, J. T., Dobry, R., Finn, W. D. L., Harder Jr., L. F., Hynes, M. E., Ishihara, K., Koester, J. P., Liao, S. S. C., Marcuson III, W. F., Martin, G. R., Mitchell, J. K., Moriwaki, Y., Power, M. S., Robertson, P. K., Seed, R. B., and Stokoe II, K. H. (2001). "Liquefaction Resistance of Soils: Summary Report from the 1996 NCEER and 1998 NCEER/NSF Workshops on Evaluation of Liquefaction Resistance of Soils", J. Geotechnical and Geoenvironmental Eng., ASCE, Vol. 127(10), 817-833.

The International Journal of Geoengineering Case Histories (IJGCH) is funded by:

Email us at main@geocasehistoriesjournal.org if your company wishes to fund the ISSMGE International Journal of Geoengineering Case Histories.